

## Measurements of $\psi(2S)$ decays to octet baryon-antibaryon pairs

M. Ablikim<sup>1</sup>, J. Z. Bai<sup>1</sup>, Y. Ban<sup>12</sup>, X. Cai<sup>1</sup>, H. F. Chen<sup>17</sup>, H. S. Chen<sup>1</sup>, H. X. Chen<sup>1</sup>, J. C. Chen<sup>1</sup>, Jin Chen<sup>1</sup>, Y. B. Chen<sup>1</sup>, Y. P. Chu<sup>1</sup>, Y. S. Dai<sup>19</sup>, L. Y. Diao<sup>9</sup>, Z. Y. Deng<sup>1</sup>, Q. F. Dong<sup>15</sup>, S. X. Du<sup>1</sup>, J. Fang<sup>1</sup>, S. S. Fang<sup>1a</sup>, C. D. Fu<sup>15</sup>, C. S. Gao<sup>1</sup>, Y. N. Gao<sup>15</sup>, S. D. Gu<sup>1</sup>, Y. T. Gu<sup>4</sup>, Y. N. Guo<sup>1</sup>, Z. J. Guo<sup>16b</sup>, F. A. Harris<sup>16</sup>, K. L. He<sup>1</sup>, M. He<sup>13</sup>, Y. K. Heng<sup>1</sup>, J. Hou<sup>11</sup>, H. M. Hu<sup>1</sup>, J. H. Hu<sup>3</sup>, T. Hu<sup>1</sup>, X. T. Huang<sup>13</sup>, X. B. Ji<sup>1</sup>, X. S. Jiang<sup>1</sup>, X. Y. Jiang<sup>5</sup>, J. B. Jiao<sup>13</sup>, D. P. Jin<sup>1</sup>, S. Jin<sup>1</sup>, Y. F. Lai<sup>1</sup>, G. Li<sup>1c</sup>, H. B. Li<sup>1</sup>, J. Li<sup>1</sup>, R. Y. Li<sup>1</sup>, S. M. Li<sup>1</sup>, W. D. Li<sup>1</sup>, W. G. Li<sup>1</sup>, X. L. Li<sup>1</sup>, X. N. Li<sup>1</sup>, X. Q. Li<sup>11</sup>, Y. F. Liang<sup>14</sup>, H. B. Liao<sup>1</sup>, B. J. Liu<sup>1</sup>, C. X. Liu<sup>1</sup>, F. Liu<sup>6</sup>, Fang Liu<sup>1</sup>, H. H. Liu<sup>1</sup>, H. M. Liu<sup>1</sup>, J. Liu<sup>12d</sup>, J. B. Liu<sup>1</sup>, J. P. Liu<sup>18</sup>, Jian Liu<sup>1</sup>, Q. Liu<sup>1</sup>, R. G. Liu<sup>1</sup>, Z. A. Liu<sup>1</sup>, Y. C. Lou<sup>5</sup>, F. Lu<sup>1</sup>, G. R. Lu<sup>5</sup>, J. G. Lu<sup>1</sup>, C. L. Luo<sup>10</sup>, F. C. Ma<sup>9</sup>, H. L. Ma<sup>2</sup>, L. L. Ma<sup>1e</sup>, Q. M. Ma<sup>1</sup>, Z. P. Mao<sup>1</sup>, X. H. Mo<sup>1</sup>, J. Nie<sup>1</sup>, S. L. Olsen<sup>16</sup>, R. G. Ping<sup>1</sup>, N. D. Qi<sup>1</sup>, H. Qin<sup>1</sup>, J. F. Qiu<sup>1</sup>, Z. Y. Ren<sup>1</sup>, G. Rong<sup>1</sup>, X. D. Ruan<sup>4</sup>, L. Y. Shan<sup>1</sup>, L. Shang<sup>1</sup>, C. P. Shen<sup>1</sup>, D. L. Shen<sup>1</sup>, X. Y. Shen<sup>1</sup>, H. Y. Sheng<sup>1</sup>, H. S. Sun<sup>1</sup>, S. S. Sun<sup>1</sup>, Y. Z. Sun<sup>1</sup>, Z. J. Sun<sup>1</sup>, X. Tang<sup>1</sup>, G. L. Tong<sup>1</sup>, G. S. Varner<sup>16</sup>, D. Y. Wang<sup>1f</sup>, L. Wang<sup>1</sup>, L. L. Wang<sup>1</sup>, L. S. Wang<sup>1</sup>, M. Wang<sup>1</sup>, P. Wang<sup>1</sup>, P. L. Wang<sup>1</sup>, Y. F. Wang<sup>1</sup>, Z. Wang<sup>1</sup>, Z. Y. Wang<sup>1</sup>, Zheng Wang<sup>1</sup>, C. L. Wei<sup>1</sup>, D. H. Wei<sup>1</sup>, U. Wiedner<sup>20</sup>, Y. Weng<sup>1</sup>, N. Wu<sup>1</sup>, X. M. Xia<sup>1</sup>, X. X. Xie<sup>1</sup>, G. F. Xu<sup>1</sup>, X. P. Xu<sup>6</sup>, Y. Xu<sup>11</sup>, M. L. Yan<sup>17</sup>, H. X. Yang<sup>1</sup>, Y. X. Yang<sup>3</sup>, M. H. Ye<sup>2</sup>, Y. X. Ye<sup>17</sup>, G. W. Yu<sup>1</sup>, C. Z. Yuan<sup>1</sup>, Y. Yuan<sup>1</sup>, S. L. Zang<sup>1</sup>, Y. Zeng<sup>7</sup>, B. X. Zhang<sup>1</sup>, B. Y. Zhang<sup>1</sup>, C. C. Zhang<sup>1</sup>, D. H. Zhang<sup>1</sup>, H. Q. Zhang<sup>1</sup>, H. Y. Zhang<sup>1</sup>, J. W. Zhang<sup>1</sup>, J. Y. Zhang<sup>1</sup>, S. H. Zhang<sup>1</sup>, X. Y. Zhang<sup>13</sup>, Yiyun Zhang<sup>14</sup>, Z. X. Zhang<sup>12</sup>, Z. P. Zhang<sup>17</sup>, D. X. Zhao<sup>1</sup>, J. W. Zhao<sup>1</sup>, M. G. Zhao<sup>1</sup>, P. P. Zhao<sup>1</sup>, W. R. Zhao<sup>1</sup>, Z. G. Zhao<sup>1g</sup>, H. Q. Zheng<sup>12</sup>, J. P. Zheng<sup>1</sup>, Z. P. Zheng<sup>1</sup>, L. Zhou<sup>1</sup>, K. J. Zhu<sup>1</sup>, Q. M. Zhu<sup>1</sup>, Y. C. Zhu<sup>1</sup>, Y. S. Zhu<sup>1</sup>, Z. A. Zhu<sup>1</sup>, B. A. Zhuang<sup>1</sup>, X. A. Zhuang<sup>1</sup>, B. S. Zou<sup>1</sup>

(BES Collaboration)

<sup>1</sup> Institute of High Energy Physics, Beijing 100049, People's Republic of China

<sup>2</sup> China Center for Advanced Science and Technology(CCAST), Beijing 100080, People's Republic of China

<sup>3</sup> Guangxi Normal University, Guilin 541004, People's Republic of China

<sup>4</sup> Guangxi University, Nanning 530004, People's Republic of China

<sup>5</sup> Henan Normal University, Xinxiang 453002, People's Republic of China

<sup>6</sup> Huazhong Normal University, Wuhan 430079, People's Republic of China

<sup>7</sup> Hunan University, Changsha 410082, People's Republic of China

<sup>8</sup> Jinan University, Jinan 250022, People's Republic of China

<sup>9</sup> Liaoning University, Shenyang 110036, People's Republic of China

<sup>10</sup> Nanjing Normal University, Nanjing 210097, People's Republic of China

<sup>11</sup> Nankai University, Tianjin 300071, People's Republic of China

<sup>12</sup> Peking University, Beijing 100871, People's Republic of China

<sup>13</sup> Shandong University, Jinan 250100, People's Republic of China

<sup>14</sup> Sichuan University, Chengdu 610064, People's Republic of China

<sup>15</sup> Tsinghua University, Beijing 100084, People's Republic of China

<sup>16</sup> University of Hawaii, Honolulu, HI 96822, USA

<sup>17</sup> University of Science and Technology of China, Hefei 230026, People's Republic of China

<sup>18</sup> Wuhan University, Wuhan 430072, People's Republic of China

<sup>19</sup> Zhejiang University, Hangzhou 310028, People's Republic of China

<sup>20</sup> Bochum University, Inst. f. Experimentalphysik I, D-44780 Bochum, Germany

<sup>a</sup> Current address: DESY, D-22607, Hamburg, Germany

<sup>b</sup> Current address: Johns Hopkins University, Baltimore, MD 21218, USA

<sup>c</sup> Current address: Universite Paris XI, LAL-Bat. 208- -BP34, 91898- ORSAY Cedex, France

<sup>d</sup> Current address: Max-Plank-Institut fuer Physik, Foehringer Ring 6, 80805 Munich, Germany

<sup>e</sup> Current address: University of Toronto, Toronto M5S 1A7, Canada

<sup>f</sup> Current address: CERN, CH-1211 Geneva 23, Switzerland

<sup>g</sup> Current address: University of Michigan, Ann Arbor, MI 48109, USA

With a sample of  $14 \times 10^6$   $\psi(2S)$  events collected by the BESII detector at the Beijing Electron Positron Collider (BEPC), the decay channels  $\psi(2S) \rightarrow B_8 \bar{B}_8$  ( $p\bar{p}$ ,  $\Lambda\bar{\Lambda}$ ,  $\Sigma^0\bar{\Sigma}^0$ ,  $\Xi^-\bar{\Xi}^+$ ) are measured, and their branching ratios are determined to be  $(3.36 \pm 0.09 \pm 0.25) \times 10^{-4}$ ,  $(3.39 \pm 0.20 \pm 0.32) \times 10^{-4}$ ,  $(2.35 \pm 0.36 \pm 0.32) \times 10^{-4}$ ,  $(2.15 \pm 0.15 \pm 0.15) \times 10^{-4}$ , and  $(1.56 \pm 0.16 \pm 0.16) \times 10^{-4}$ , respectively. The measured branching ratios are in agreement with the theoretical predictions.

## 1. Introduction

The branching ratios of  $\psi(2S)$  decays into octet baryon-antibaryon pairs were measured by the BES-I and CLEOc collaborations, and the results differ significantly, as shown in Table 1. It is therefore important to make new measurements to help clarify these differences using the sample of  $14 \times 10^6$   $\psi(2S)$  events collected by BESII, which is the world's largest  $e^+e^- \psi(2S)$  sample.

Table 1  
Branching ratios of  $\psi(2S) \rightarrow B_8 \bar{B}_8 (\times 10^{-4})$ .

Channel	BES-I [1]	CLEO-c [2]
$p\bar{p}$	$2.16 \pm 0.15 \pm 0.36$	$2.87 \pm 0.12 \pm 0.15$
$\Lambda\bar{\Lambda}$	$1.81 \pm 0.20 \pm 0.27$	$3.28 \pm 0.23 \pm 0.25$
$\Sigma^0\bar{\Sigma}^0$	$1.2 \pm 0.4 \pm 0.4$	$2.63 \pm 0.35 \pm 0.21$
$\Xi^-\bar{\Xi}^+$	$0.94 \pm 0.27 \pm 0.15$	$2.38 \pm 0.30 \pm 0.21$

According to the hadron helicity conservation, the angular distribution of  $\psi(2S) \rightarrow B_8 \bar{B}_8$  can be expressed as:

$$\frac{dN}{d\cos\theta} \propto 1 + \alpha \cos^2\theta, \quad (1)$$

where  $\theta$  is the angle between  $B_8$  and the beam direction of the positron in the center-of-mass (CM) system. In the limit of infinitely heavy charm mass, hadron helicity conservation implies  $\alpha = 1$  [3] for both  $J/\psi$  and  $\psi(2S)$  decays to octet baryon anti-baryon pairs.

Values of  $\alpha$  for  $J/\psi$ ,  $\psi(2S) \rightarrow p\bar{p}$  have been predicted theoretically based on first order QCD. In the prediction of Claudson, Glashow, and Wise [4], the mass of the final baryon is taken into account as a whole, while the constituent quarks inside the baryon are taken as massless when computing the decay amplitude. In the prediction by Carimalo [5], mass effects at the quark level are taken into consideration. Experimentally there

are several measurements for  $\alpha$  for  $J/\psi \rightarrow p\bar{p}$ , and the recent result of  $\alpha = 0.676 \pm 0.036 \pm 0.042$  given by BES [6] is quite close to Carimalo's prediction  $\alpha = 0.69$  [5]. However, there is only one measurement for  $\psi(2S) \rightarrow p\bar{p}$ , made by E835 [7]. Results for  $\psi(2S) \rightarrow p\bar{p}$  are summarized in Table 2. The  $\psi(2S) \rightarrow p\bar{p}$  events in BESII allow the measurement of  $\alpha$ , which can be compared with the existing result and used to test hadron helicity conservation.

Table 2  
Predicted and measured values of  $\alpha$  for  $\psi(2S) \rightarrow p\bar{p}$ .

$\alpha$ value	Source
Predicted value:	
$\alpha = 0.58$	Claudson <i>et al.</i> [4]
$\alpha = 0.80$	Carimalo [5]
Measured value:	
$\alpha = 0.67 \pm 0.15 \pm 0.04$	M. Ambrogiani <i>et al.</i> [7]

BESII is a large solid-angle magnetic spectrometer which is described in detail in Ref. [8]. The momentum of charged particles is determined by a forty-layer cylindrical main drift chamber (MDC) which has a resolution of  $\sigma_p/p = 1.78\% \sqrt{1 + p^2}$  ( $p$  in  $\text{GeV}/c$ ). Particle identification is accomplished using specific ionization ( $dE/dx$ ) measurements in the drift chamber and time-of-flight (TOF) information in a barrel-like array of forty-eight scintillation counters. The  $dE/dx$  resolution is  $\sigma_{dE/dx} \simeq 8.0\%$ ; the TOF resolution for Bhabha events is  $\sigma_{TOF} = 180$  ps. Radially outside of the time-of-flight counters is a 12-radiation-length barrel shower counter (BSC) comprised of gas tubes interleaved with lead sheets. The BSC measures the energy and direction of photons with resolutions of  $\sigma_E/E \simeq 21\%/\sqrt{E}$  ( $E$  in  $\text{GeV}$ ),  $\sigma_\phi = 7.9$  mrad,

and  $\sigma_z = 2.3$  cm. The iron flux return of the magnet is instrumented with three double layers of proportional counters that are used to identify muons.

Monte Carlo (MC) simulation is used for mass resolution and detection efficiency determination. In this analysis, a GEANT3 [9] based MC package (SIMBES) with detailed consideration of the detector performance (such as dead electronic channels) is used. The consistency between data and MC has been carefully checked in many high purity physics channels, and the agreement is reasonable [10].

The data samples used for this analysis consist of  $14.0 \times 10^6 (1 \pm 4\%)$   $\psi(2S)$  events [11] and  $6.42(1 \pm 4\%) \text{ pb}^{-1}$  of continuum data at  $\sqrt{s} = 3.65 \text{ GeV}$  [12]. The decay channels investigated are  $\psi(2S) \rightarrow p\bar{p}$ ,  $\Lambda\bar{\Lambda}$ ,  $\Sigma^0\bar{\Sigma}^0$ , and  $\Xi^-\bar{\Xi}^+$ , where  $\Lambda$  decays to  $p\pi^-$  (63.9%),  $\Sigma^0$  decays to  $\Lambda\gamma$  (100%), and  $\Xi^-$  decays to  $\Lambda\pi^-$  (99.9%).

## 2. Event selection and branching ratio determination

### 2.1. $\psi(2S) \rightarrow p\bar{p}$

The experimental signature for the decay  $\psi(2S) \rightarrow p\bar{p}$  is two back-to-back, oppositely-charged tracks, each with a momentum of  $1.586 \text{ GeV}/c$ . The main backgrounds are: Bhabha and dimuon ( $e^+e^- \rightarrow \mu^+\mu^-$ ) events,  $\psi(2S) \rightarrow e^+e^-$ ,  $\mu^+\mu^-$ ,  $\pi^+\pi^-$ ,  $K^+K^-$ ,  $\psi(2S) \rightarrow \gamma\chi_{CJ(J=0,1,2)} \rightarrow \gamma\pi^+\pi^-$  ( $K^+K^-$ ,  $p\bar{p}$ ),  $\psi(2S) \rightarrow \pi^0\pi^0J/\psi \rightarrow \pi^0\pi^0e^+e^-$  ( $\mu^+\mu^-$ ),  $\psi(2S) \rightarrow \pi^0p\bar{p}$ , etc.

The event selection requires two well reconstructed and oppositely charged tracks. Each track is required to be well fitted to a three dimensional helix, be in the polar angle region  $|\cos\theta| < 0.8$ , and have a momentum greater than  $70 \text{ MeV}/c$  in the  $xy$ -plane. The point of closest approach of each track to the beamline is required to be within the interaction region which

is defined to be  $\pm 20 \text{ cm}$  longitudinally and  $2 \text{ cm}$  radially.

In order to remove cosmic rays, the difference between the time-of-flights of the positive and negative tracks,  $|t_+ - t_-|$ , is required to be less than  $4.0 \text{ ns}$ . Protons and antiprotons are required to be identified by the TOF; the measured time-of-flight of the track must be closest to the prediction for the proton/anti-proton hypothesis. Since  $\psi(2S) \rightarrow p\bar{p}$  is a back-to-back two-body decay, we require the acollinearity angle of two tracks to be less than  $5^\circ$ . The deposited energy in the BSC of the positive particle is required to be less than  $0.75 \text{ GeV}$  to remove possible  $e^+e^-$  final state contamination. Finally, the energy sum (calculated from the track's momentum) of the two tracks is required to be within  $130 \text{ MeV}$  of the expected sum,  $3.686 \text{ GeV}$ , and the momentum of the negative track is required to be within  $150 \text{ MeV}/c$  of the expected momentum  $1.586 \text{ GeV}/c$ .

Events surviving the selection criteria are shown in Fig. 1 as dots with error bars. The same selection criteria have been applied to background events generated by the MC and normalized according to branching ratios listed in PDG(2006) [13], and 38.1 background events survive and are shown as the dashed line in Fig. 1. The data are fitted by a MC histogram for the signal plus a background function which corresponds to the 38.1 simulated background events and a flat distribution to describe the remaining background. From the fit, the number of  $p\bar{p}$  events is determined to be  $1618.2 \pm 43.4$ , where the error is statistical.

#### 2.1.1. Angular distribution of $p\bar{p}$

To obtain the parameter  $\alpha$  for  $\psi(2S) \rightarrow p\bar{p}$ , the  $\cos\theta$  dependence of the event selection efficiency must be taken into account, which is determined using a flat angular distribution ( $\alpha=0$ ) in the MC simulation; see Fig. 2(a). However, there are imperfections in the MC simulation, which will dis-

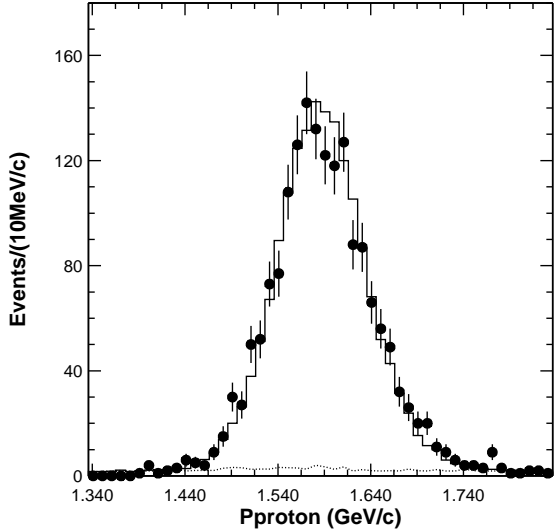


Figure 1. The fitted proton momentum spectrum. The dots with error bars are data, the histogram is the fit to the data including the signal shape from MC and all backgrounds, and the dashed line is the background.

tort the efficiencies determined by the MC as a function of  $\cos\theta$ . In order to reduce this systematic error, a correction to the MC efficiency is made [6]. The correction factor  $f_c(\cos\theta)$  is defined as:

$$f_c(\cos\theta) = \frac{\varepsilon_{Data}}{\varepsilon_{MC}}(\cos\theta) = \prod_i \frac{\varepsilon_{Data}(i)}{\varepsilon_{MC}(i)}(\cos\theta),$$

where  $i$  denotes the selection criterion,  $\varepsilon_{Data}(i)$  is the efficiency determined for data for criterion  $i$ , and  $\varepsilon_{MC}(i)$  is the efficiency from the MC for criterion  $i$ . The corrected MC efficiency is then:

$$\varepsilon'_{MC}(\cos\theta) = \varepsilon_{MC}(\cos\theta) \times f_c(\cos\theta).$$

Due to the limitation on the number of  $\psi(2S) \rightarrow p\bar{p}$  events, the "reference" channel  $J/\psi \rightarrow p\bar{p}$  is chosen to determine the correction factor due to its higher statistics and similar kinematics. The selection criteria related to

the energy and momentum for  $\psi(2S) \rightarrow p\bar{p}$  are scaled to the reference channel  $J/\psi \rightarrow p\bar{p}$ . Then following the re-weighting procedures in Ref. [6] for our selection criteria, the correction function  $f_c(\cos\theta)$  is obtained and is shown in Fig. 2(c). With  $\varepsilon_{MC}(\cos\theta)$  denoting the efficiency obtained from  $\psi(2S) \rightarrow p\bar{p}$  MC and  $f_c(\cos\theta)$  the correction function for the efficiency, we fit the measured angular distribution of  $\psi(2S) \rightarrow p\bar{p}$  data with the function  $N(\cos\theta)$ ,

$$N(\cos\theta) = N_0 \times (1 + \alpha \cos^2\theta) \times \varepsilon_{MC}(\cos\theta) \times f_c(\cos\theta),$$

as shown in Fig. 2(d). The fit uses a binned  $\chi^2$  minimization method in the angular range  $\cos\theta \in [-0.7, 0.7]$  and gives  $\chi^2_{min} = 10.88$  for 12 degrees of freedom. The fitted value of the parameter  $\alpha$  is  $0.85 \pm 0.24$ , where the error is statistical.

As a consistency check, we also obtained  $f_c(\cos\theta)$  directly from the  $\psi(2S) \rightarrow p\bar{p}$  sample, and the fitted result obtained using this correction yields  $\alpha = 0.83 \pm 0.24$ , but its systematic uncertainty is 0.14, mainly due to the lower statistics of the  $\psi(2S) \rightarrow p\bar{p}$  sample, and much larger than the systematic error of 0.04 determined using  $f_c(\cos\theta)$  obtained from the  $J/\psi \rightarrow p\bar{p}$  sample (see section 3.1). This demonstrates that  $f_c(\cos\theta)$  determined from the  $J/\psi \rightarrow p\bar{p}$  sample improves the systematic error on  $\alpha$  without changing its central value and statistical error.

### 2.1.2. Branching ratio of $\psi(2S) \rightarrow p\bar{p}$

The selection efficiency is determined using  $1 \times 10^5 \psi(2S) \rightarrow p\bar{p}$  MC events. The MC-determined efficiency is  $\varepsilon_{MC} = (34.4 \pm 0.2)\%$ , and the branching ratio is determined to be:

$$Br(\psi(2S) \rightarrow p\bar{p}) = (3.36 \pm 0.09) \times 10^{-4},$$

where the error is statistical.

### 2.2. $\psi(2S) \rightarrow \Lambda\bar{\Lambda}$

Candidate events require four well reconstructed charged tracks. The positive (negative)

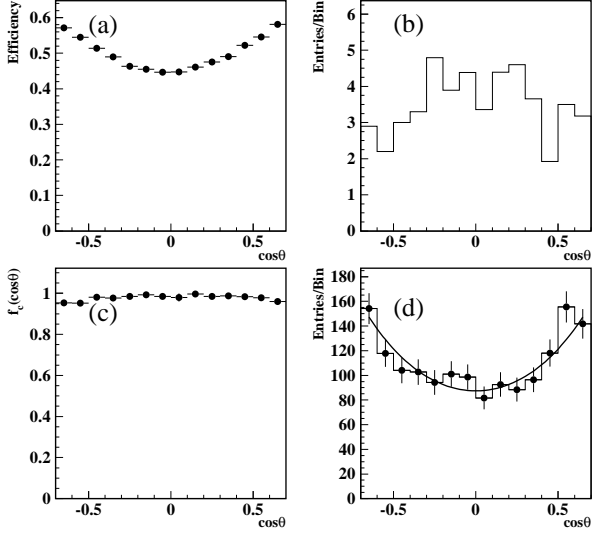


Figure 2. (a) The selection efficiency versus  $\cos\theta$  obtained from MC; (b) angular distribution of background events from MC, which survive the same selection criteria as used for data; (c) the correction obtained from data ( $f_c(\cos\theta)$ ) to the MC efficiency; and (d) the angular distribution of candidate  $\psi(2S) \rightarrow p\bar{p}$  events.

charged track with the higher momentum is assumed to be the proton (antiproton); the other two are assumed to be the  $\pi^+$  and  $\pi^-$ . The two  $p\pi$  pairs are required to pass the  $\Lambda$ 's vertex finding algorithm successfully, and the sum of the  $\Lambda$  and  $\bar{\Lambda}$  decay lengths must be greater than 0.02 m (see Fig. 3). The sum of the  $\Lambda$  and  $\bar{\Lambda}$  energies must be in the region from 3.60 GeV to 3.81 GeV (see Fig. 4). The missing momentum of the events should be less than 0.18 GeV/ $c$ , and the difference between the measured mass of  $M_{\bar{p}\pi^+}$  and its expected value,  $M_\Lambda$ , should be less than 12 MeV/ $c^2$  (three times the resolution of the  $M_\Lambda$ ).

The events that satisfy the selection criteria are shown in Fig. 5 as dots with error bars; they are fitted by a histogram of the signal shape from

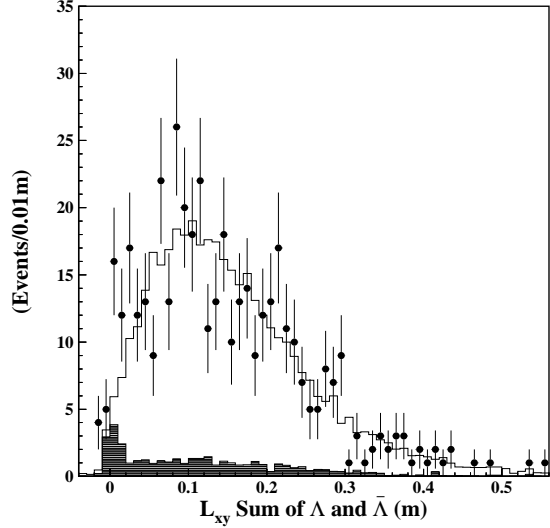


Figure 3. The sum of the  $\Lambda$  and  $\bar{\Lambda}$  decay lengths. The histogram is the signal shape from the MC plus simulated background, the dots with error bars are data, and the shaded histogram is the background.

MC plus a background function which describes the simulated backgrounds and a flat distribution to describe any remaining sources. The simulated backgrounds are mainly from  $\psi(2S) \rightarrow \Sigma^0 \bar{\Sigma}^0$  and  $\psi(2S) \rightarrow \Lambda \bar{\Sigma}^0 + c.c.$  and normalizing according to branching ratios from PDG(2006), a total of 32 background events are obtained. The final number of signal events from the fit is  $337.2 \pm 19.9$ .

The  $\psi(2S) \rightarrow \Lambda \bar{\Lambda} \rightarrow p\bar{p}\pi^+\pi^-$  efficiency is determined to be  $\epsilon_{MC} = (17.4 \pm 0.2)\%$  using  $2 \times 10^5$  MC-simulated signal events. The branching ratio is then:

$$Br(\psi(2S) \rightarrow \Lambda \bar{\Lambda}) = (3.39 \pm 0.20) \times 10^{-4},$$

where the error is statistical.

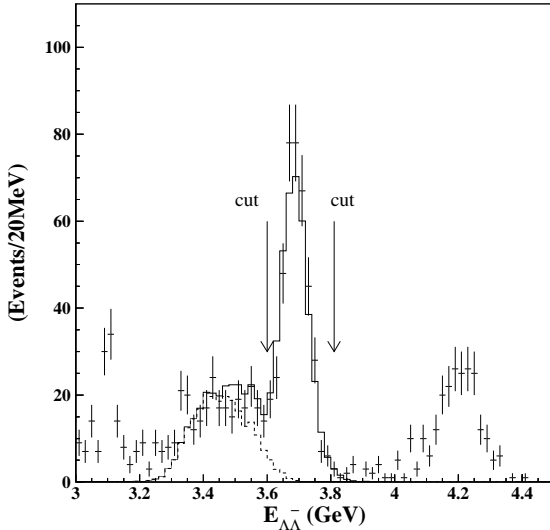


Figure 4. The sum of the  $\Lambda$  and  $\bar{\Lambda}$  energies. The histogram is the signal shape from the MC plus backgrounds. The dots with error bars are data, and the dashed line is the main background from  $\psi(2S) \rightarrow \Sigma^0 \bar{\Sigma}^0$ . The peaks at 3.1 and 4.2 GeV are from  $\psi(2S) \rightarrow \pi^0 \pi^0 J/\psi$ ,  $J/\psi \rightarrow \Lambda \bar{\Lambda}$  and  $\psi(2S) \rightarrow \pi^+ \pi^- J/\psi$ ,  $J/\psi \rightarrow e^+ e^-$  (or  $\mu^+ \mu^-$ ), respectively.

### 2.3. $\psi(2S) \rightarrow \Sigma^0 \bar{\Sigma}^0$

Candidate events are required to have four well reconstructed charged tracks plus at least two good photons. The  $\Lambda$  and  $\bar{\Lambda}$  are selected using the method described in Section B. The missing momentum of the events is required to be less than  $0.25 \text{ GeV}/c$ . The  $\chi^2$  of the four constraint (4C) kinematic fit to the hypothesis  $\psi(2S) \rightarrow p\bar{p}\pi^+\pi^-\gamma\gamma$  must be less than 20. The difference between the measured mass of  $M_{\bar{p}\pi^+\gamma}$  and its expected value,  $M_{\bar{\Sigma}^0}$ , should be less than  $36 \text{ MeV}/c^2$  (three times the  $M_{\bar{\Sigma}^0}$  resolution).

The events that survive selection are shown in Fig. 6 as dots with error bars; they are fitted by a histogram of the signal shape from MC

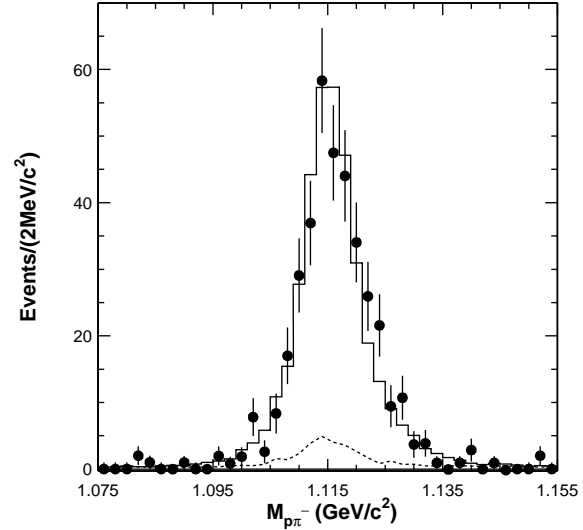


Figure 5. The fitted  $\Lambda$  mass spectrum. The dots with error bars are data, the histogram is the fit to data which includes the signal shape from MC plus all backgrounds, and the dashed line is the background.

plus a background function which describes the simulated backgrounds and a flat distribution to describe the remaining background. The main backgrounds are from  $\psi(2S) \rightarrow \Lambda \bar{\Lambda}$ ,  $\psi(2S) \rightarrow \gamma \chi_{CJ(J=0,1,2)} \rightarrow \gamma \Lambda \bar{\Lambda}$ ,  $\psi(2S) \rightarrow \Xi^0 \bar{\Xi}^0$ ,  $\psi(2S) \rightarrow \Lambda \bar{\Sigma}^0 + c.c.$  and  $\psi(2S) \rightarrow \Sigma^0 \bar{\Xi}^0 + c.c.$ , and normalizing using branching ratios from PDG(2006), 16.5 background events are obtained. The final number of signal events from the fit is  $59.1 \pm 9.1$ .

The  $\psi(2S) \rightarrow \Sigma^0 \bar{\Sigma}^0 \rightarrow \Lambda \bar{\Lambda} \gamma\gamma \rightarrow p\bar{p}\pi^+\pi^-\gamma\gamma$  efficiency is determined to be  $\epsilon_{MC} = (4.4 \pm 0.1)\%$  using  $2 \times 10^5$  MC generated signal events. The branching ratio of signal channel is then:

$$Br(\psi(2S) \rightarrow \Sigma^0 \bar{\Sigma}^0) = (2.35 \pm 0.36) \times 10^{-4},$$

where the error is statistical.

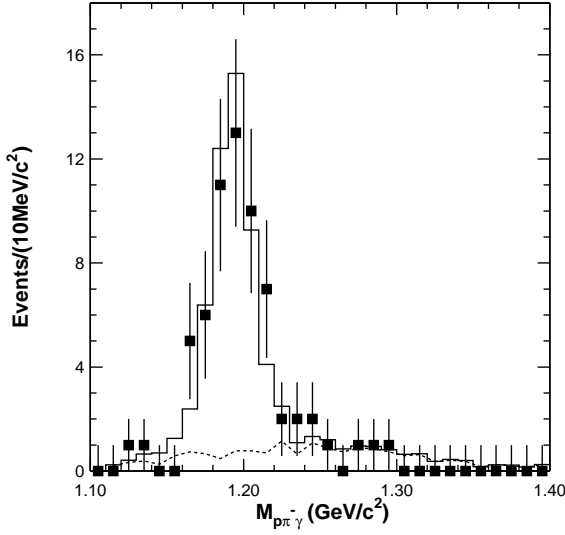


Figure 6. The fitted  $\Sigma^0$  mass spectrum. The dots with error bars are data, the histogram is the fit to data which includes the signal shape from the MC and all backgrounds, and the dashed line is the background.

#### 2.4. $\psi(2S) \rightarrow \Xi^- \bar{\Xi}^+$

Candidate events require six well reconstructed charged tracks. The positive (negative) charged track with highest momentum is assumed to be the proton (antiproton); the other four are assumed to be  $\pi$ s. Looping over all possible  $p\pi^-$ ,  $\bar{p}\pi^+$  combinations in an event, the one which successfully passes the vertex finding algorithm and has the smallest value of  $\sqrt{(M_{p\pi^-} - M_\Lambda)^2 + (M_{\bar{p}\pi^+} - M_{\bar{\Lambda}})^2}$  is selected for further analysis. The energy sum of the  $\Xi^-$  and  $\bar{\Xi}^+$  should be between 3.593 and 3.779 GeV (see Fig. 7), and the missing momentum of the events should be less than 0.15 GeV/ $c$ . The difference between the measured mass of  $M_{\bar{p}\pi^+\pi^-}$  and its expected value,  $M_{\Xi^-}$ , should be less than 18 MeV/ $c^2$  (three times the  $M_{\Xi^-}$  resolution).

The events surviving selection are shown in

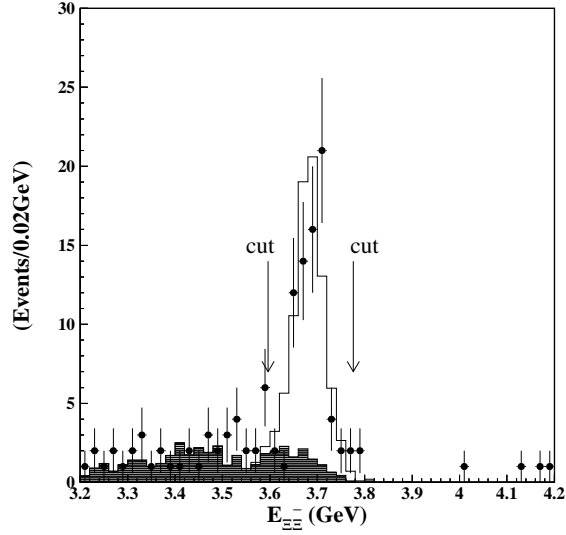


Figure 7. The  $\Xi^-$  and  $\bar{\Xi}^+$  energy sum. The histogram is the signal shape from MC plus background. The dots with error bars are data, and the shaded area is the sum of simulated backgrounds.

Fig. 8 as dots with error bars, and they are fitted by a histogram of the signal shape from MC plus a background function which describes the simulated backgrounds and a flat distribution to describe remaining background. The main background is from  $\psi(2S) \rightarrow \pi^+\pi^- J/\psi \rightarrow \pi^+\pi^-\Lambda\bar{\Lambda}$ , and normalizing by PDG(2006) branching fractions, 11.3 background events are obtained. The final number of signal events from the fit is  $67.4 \pm 8.9$ .

The  $\psi(2S) \rightarrow \Xi^- \bar{\Xi}^+ \rightarrow \Lambda\bar{\Lambda}\pi^+\pi^- \rightarrow p\bar{p}\pi^+\pi^-\pi^+\pi^-$  efficiency is determined to be  $\epsilon_{MC} = (3.9 \pm 0.1)\%$  using  $2 \times 10^5$  signal events generated by MC. The branching ratio of the signal channel is then:

$$Br(\psi(2S) \rightarrow \Xi^- \bar{\Xi}^+) = (3.03 \pm 0.40) \times 10^{-4},$$

where the error is statistical.

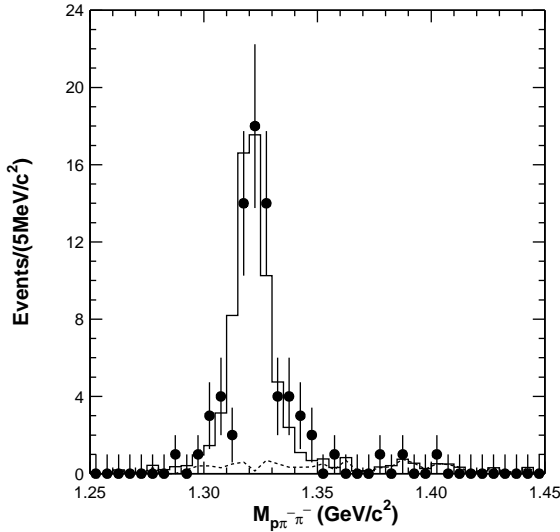


Figure 8. The fitted  $\Xi^-$  mass spectrum. Dots with error bars are data, the histogram is the fit to data which includes the signal shape from the MC and all backgrounds, and the dashed line is the sum of the backgrounds.

### 3. Systematic error

#### 3.1. $\psi(2S) \rightarrow p\bar{p}$ angular distribution

The systematic error on  $\alpha$  in  $\psi(2S) \rightarrow p\bar{p}$  decay from the tracking reconstruction is determined using different MDC wire resolution models in the MC simulations, which changes  $\alpha$  by 2.7%. When the fit parameter of the efficiency correction curve  $f_c(\cos\theta)$  is changed by  $1\sigma$ ,  $\alpha$  changes by 2.3%. The performance of the BES detector has small differences between the time when the  $58 \times 10^6$   $J/\psi$  events were obtained and when the  $14 \times 10^6$   $\psi(2S)$  events were obtained. Using parameter files describing the performance of BES detector at these two data taking periods, the effect of this variation on  $\alpha$  is determined to be 2.2%. The effect of the background uncertainty on  $\alpha$  is negligible. Adding these contributions in

quadrature gives a total systematic error of 4.2%.

#### 3.2. Branching ratios

The systematic errors on the branching ratios are mainly from the uncertainties in the MDC tracking,  $\alpha$ , the hadronic interaction model, background estimations, and differences between data and MC for the  $\Lambda$  vertex finding, decay length requirement, and kinematic fitting.

The MDC tracking gives a systematic error of about 2% for a proton or anti-proton [10] and 1% for a low-energy  $\pi$ , which is determined from the channel  $\psi(2S) \rightarrow \pi^+ \pi^- J/\psi \rightarrow \pi^+ \pi^- \mu^+ \mu^-$ . The detection efficiency depends on the angular distribution of the baryon pair. For  $p\bar{p}$  decay, when changing the  $\alpha$  value by  $1\sigma$ , the branching ratio changes by 2.4%; in the other three channels,  $\alpha = 0.5$  is used as a nominal value, the maximum differences for  $|\epsilon_{\alpha=0.5} - \epsilon_{\alpha=0}|$  and  $|\epsilon_{\alpha=0.5} - \epsilon_{\alpha=1}|$  are taken as systematic errors, they are 6.5%, 7.6%, 6.8%, respectively. The uncertainties of the detection efficiencies caused by assumed flat angular distributions for secondary decay of baryons are much smaller than those from angular distributions of  $\psi(2S)$  to baryon pair primary decays, and are therefore neglected here [14]. Different simulation models for the hadronic interaction (GCALOR/Geant-FLUKA) [15,16] give different efficiencies, giving systematic errors of 2.18%, 0.46%, 0.00%, 1.08% for the studied channels, respectively. The background uncertainty is studied by changing the nominal branching ratios of the backgrounds which have large statistical errors. If the branching ratios of the background channels are changed by 100% in the  $p\bar{p}$ ,  $\Lambda\bar{\Lambda}$ , and  $\Xi^-\bar{\Xi}^+$  channels, the changes in the branching ratios in the signal channels are 0.1%, 1.0% and 0.2%, respectively. For the  $\Sigma^0\bar{\Sigma}^0$  channel, where the shape of the simulated backgrounds is in good agreement with the data in the  $\Lambda\gamma$  invariant mass distribution, the branching ratios of backgrounds are only changed by 20%, resulting

in a change of the branching ratios of the signal channel of 2.3%. According to the reference channel  $J/\psi \rightarrow \Lambda\bar{\Lambda}$  [17], the secondary vertex finding of  $\Lambda$  gives a systematic error of 0.7% for each  $\Lambda$  vertex, and the requirement on the sum of the decay length contributes 1.4%.

In the branching ratio determination of four channels, the continuum contribution must be subtracted. The continuum data are also selected with the same criteria as for the  $\psi(2S)$  decay signal channels, and the number of the surviving events times a luminosity normalization factor is taken as a systematic error. The kinematic fit of  $p\bar{p}\pi^+\pi^-\gamma\gamma$  in  $\psi(2S) \rightarrow \Sigma^0\bar{\Sigma}^0$  gives a systematic error of 7.6% from the reference channel  $\psi(2S) \rightarrow \pi^+\pi^-J/\psi \rightarrow \pi^+\pi^-\pi^+\pi^-\pi^0$  [18]. The uncertainty on the total number of  $\psi(2S)$  events is 4%. The systematic errors of the acollinearity angle,  $E_{B\bar{B}}$  region, baryon mass (or momentum), and  $P_{miss}$  requirements are studied with corresponding  $J/\psi \rightarrow p\bar{p}$  decays.

In the  $\psi(2S) \rightarrow p\bar{p}$  selection, the systematic errors due to the uncertainties from particle identification, the cosmic ray veto, and the deposited energy criterion are studied by this channel itself. All the systematic errors in the branching ratio measurements are summarized in Table 3.

#### 4. Summary and discussion

Based on  $14 \times 10^6$   $\psi(2S)$  events, the branching ratios of  $\psi(2S) \rightarrow p\bar{p}$ ,  $\Lambda\bar{\Lambda}$ ,  $\Sigma^0\bar{\Sigma}^0$ , and  $\Xi^-\bar{\Xi}^+$  are measured, the results are listed in Table 4, together with the ratios of  $\psi(2S) \rightarrow B\bar{B}$  to  $J/\psi \rightarrow B\bar{B}$ . They are in agreement with the results published by the CLEO collaboration [2] within  $2\sigma$  for  $p\bar{p}$  and within  $1\sigma$  for the other three channels. The differences of the branching fractions between current measurements and those of BESI are  $2.5\sigma$ ,  $3.1\sigma$ ,  $1.5\sigma$ ,  $3.5\sigma$  for the four channels, respectively.

The angular distribution parameter  $\alpha$  for

$\psi(2S) \rightarrow p\bar{p}$  is measured to be  $0.85 \pm 0.24 \pm 0.04$ , which is in agreement within  $1\sigma$  with the E835 result [7], and close to Carimalo's prediction [5].

Table 3

Systematic errors in the branching ratio measurements (%).

Source	$p\bar{p}$	$\Lambda\bar{\Lambda}$	$\Sigma^0\bar{\Sigma}^0$	$\Xi^-\bar{\Xi}^+$
MDC tracking	4	4.5	4.5	5.7
PID	2.4			
Cosmic Ray Exc.	0.9			
Deposit Energy	0.9			
Acol. angle	0.9			
Vtx. finding		1.4	1.4	1.4
Decay length		1.0	1.0	
$E_{B\bar{B}}$ , $M_B$ (or $P_B$ )	0.8	0.6	1.6	1.6
$P_{miss}$		1.6	0.5	1.7
$\gamma$ tracking			4	
Kinematic fit			7.6	
Bg. Esti.		1.0	2.3	0.2
Continuum data	0.8	1.0		
$\alpha$ value	2.4	6.5	7.6	6.8
Hadronic Interaction	2.2	0.5		1.1
$N_{\psi(2S)}$	4	4	4	4
Total error	7.3	9.4	13.4	10.3

#### 5. Acknowledgement

The BES collaboration thanks the staff of BEPC for their hard efforts. This work is supported in part by the National Natural Science Foundation of China under contracts Nos. 10491300, 10225524, 10225525, 10425523, the Chinese Academy of Sciences under contract No. KJ 95T-03, the 100 Talents Program of CAS under Contract Nos. U-11, U-24, U-25, and the Knowledge Innovation Project of CAS under Contract Nos. U-602, U-34 (IHEP), the National Natural Science Foundation of China under

Table 4

Branching ratios of  $\psi(2S)$  decays into baryon anti-baryon pairs. The first error is statistical and the second systematic. The value Q is  $BR(\psi(2S) \rightarrow B\bar{B})/BR(J/\psi \rightarrow B\bar{B})$ . The  $J/\psi$  branching ratios are taken from Ref. [6] for  $p\bar{p}$ , Ref. [17] for  $\Lambda\bar{\Lambda}$  and  $\Sigma^0\bar{\Sigma}^0$ , and Ref. [13] for  $\Xi^-\bar{\Xi}^+$ .

modes	BRs ( $\times 10^{-4}$ )	Q (%)
$p\bar{p}$	$3.36 \pm 0.09 \pm 0.25$	$14.9 \pm 1.4$
$\Lambda\bar{\Lambda}$	$3.39 \pm 0.20 \pm 0.32$	$16.7 \pm 2.1$
$\Sigma^0\bar{\Sigma}^0$	$2.35 \pm 0.36 \pm 0.32$	$16.8 \pm 3.6$
$\Xi^-\bar{\Xi}^+$	$3.03 \pm 0.40 \pm 0.32$	$16.8 \pm 4.7$

Contract No. 10225522 (Tsinghua University), and the Department of Energy under Contract No. DE-FG02-04ER41291 (U Hawaii).

## REFERENCES

1. J. Z. Bai *et al.* (BES Collab.), Phys. Rev. **D 63**, 032002 (2001).
2. T. K. Pedlar *et al.* (CLEO Collab.), Phys. Rev. **D 72**, 051108 (2005).
3. S.J.Brodsky and G.P.Lepage, Phys. Rev. **D 24**, 2848 (1981).
4. M. Claudson, S.L. Glashow and M.B.Wise, Phys. Rev. **D 25**, 1345 (1982).
5. C. Carimalo (College de France), Int. J. Mod. Phys. **A 2**, 249 (1987).
6. J. Z. Bai *et al.* (BES Collab.), Phys. Lett. **B 591**, 42 (2004).
7. M. Ambrogiani *et al.* (E835 Collab.), Phys. Lett. **B 610**, 177 (2005).
8. J. Z. Bai *et al.* (BES Collab.), Nucl. Inst. and Meths. **A 458**, 627 (2001).
9. CERN Application Software Group, GEANT-Detector Description and Simulation Tool, CERN Program Library Long Writeup **W 5013**, Geneva(1994).
10. M. Ablikim *et al.* (BES Collab.), Nucl. Inst. and Meths. **A 552**, 344 (2005).
11. X. H. Mo *et al.*, HEP & NP **28**, 455 (2004).
12. S. P. Chi, X. H. Mo and Y. S. Zhu, Measurement of the Integrated Luminosity at  $\sqrt{s} = 3.65, 3.686$  GeV.
13. W. M. Yao *et al.*, J. Phys. G **33**, 1 (2006).
14. R. G. Ping, H. B. Li, HEP & NP, 30 (09), 819 (2006).
15. C. Zeitnitz and T. A. Gabriel, Nucl. Inst. and Meths. **A 349**, 106 (1994).
16. K. Hansgen, H. J. Mohring and J. Ranft, Nucl. Sci. Eng. **88**, 551 (1984); J. Ranft and S. Ritter, Zeit. Physik **C 20**, 347 (1983); A. Fasso *et al.*, FLUKA 92, Proceedings of the Workshop on Simulating Accelerator Radiation Environment, Santa Fe(1993).
17. M. Ablikim *et al.* (BES Collab), Phys. Lett. **B 632**, 181 (2006).
18. M. Ablikim *et al.* (BES Collab), Phys. Lett. **B 619**, 247 (2005); J. Z. Bai *et al.* (BES Collab.), Phys. Rev. **D 70**, 012005 (2004).